*Journal of Applied Fluid Mechanics*, Vol. 17, No. 12, pp. 2533-2544, 2024.
Available online at www.jafmonline.net, ISSN 1735-3572, EISSN 1735-3645.
https://doi.org/10.47176/jafm.17.12.2794

# Experimental Performance Study of a Transcritical $CO_2$ Heat Pump Equipped with a Passive Ejector

K. Ameur† and M. Falsafioon

*CanmetENERGY, Natural Resources Canada, Varennes, Qc, J3X 1P7, Canada*

†*Corresponding Author Email: khaled.ameur@NRCan-RNCan.gc.ca*

## ABSTRACT

This study is dedicated to an experimental investigation of a passive two-phase ejector used as an expander in a transcritical $CO_2$ heat pump. The investigation focused on the impact of the evaporating temperature ($T_{evap}$) and the $CO_2$ gas cooler outlet temperature ($T_{gc\text{-}out}$) on the ejector and the overall cycle performance. The basic cycle without an ejector was also tested as a baseline for comparison. Two ejectors designed with different modeling approaches were tested and compared. The ejector with an enlarged mixing section diameter was selected for subsequent testing due to its improved pressure lift. The optimum primary nozzle position was found to be 4 times the mixing section diameter ($D_{mix}$). Although the ejector was designed for specific conditions, the results demonstrate its ability to remain operational under varying conditions with some changes in performance. The ejector's performance was observed to be dependent on the $T_{evap}$, and particularly on the $T_{gc\text{-}out}$. The pressure lift recorded was in the range of 3.7-6.5 bar, and the lowest value was obtained with the low $T_{gc\text{-}out}$ value (29 °C). Under the tested conditions, the integration of the ejector enhances the performance and the capacity of the heat pump. The ejector cycle improvement is primarily based on improved mass flow rates due to increased compressor suction pressure, reduced compression ratio, and consequently, improved compressor operating conditions. Improvements of up to 18% in heating COP and 20.5% in heating capacity were observed. The study provides valuable insights into enhancing the performance of transcritical $CO_2$ heat pump system by refining ejector design. It explores the behavior of the system across varying conditions, highlighting the significant impact of the ejector-compressor interaction on overall performance.

***Article History***

*Received April 15, 2024*
*Revised June 30, 2024*
*Accepted July 18, 2024*
*Available online October 2, 2024*

***Keywords:***

*Experiments*
*Heat-pump*
*Natural refrigerant*
*Ejector-compressor interaction*

## 1. INTRODUCTION

The adoption of carbon dioxide, a natural refrigerant with minimal impact on global warming, in mechanical compression cycles, stands as a solution to the current climate crisis. This eco-friendly approach aligns harmoniously with global initiatives to enhance energy efficiency and diminish reliance on fossil fuels.

Technology and knowledge regarding $CO_2$ systems are continuously evolving, and their adoption in different applications is likely to increase, including but not limited to refrigeration systems (Barta et al., 2021), heat pump systems (Badache et al., 2018; Song et al., 2022), and the transcritical Rankine cycle for power generation (Sarkar, 2015). For instance, in supermarket applications, the transcritical $CO_2$ booster system based on a two-stage compressor cycle is a well-established technology (Arpagaus et al., 2016). And the $CO_2$ heat pump (HP) for water heating demonstrates a promising potential in both residential and industrial sectors (Zhang et al., 2015; Wang et al., 2022).

The systems employing transcritical $CO_2$ experience significant exergy degradation during the expansion valve's throttling process (Liu et al., 2021), leading to a decrease in overall performance. To mitigate this issue and recover a part of the work lost during the expansion process, various types of expanders, including piston, rotary scroll, and turbomachine, have been evaluate (Zhang et al., 2015; Elbel & Lawrence, 2016; Ferrara et al., 2016;). Nevertheless, the low efficiencies due to friction induced by the moving components, and the refrigerant leakage issues generally counterbalance the potential advantages yielded by this category of equipment. The pressure exchanger (Sengupta & Dasgupta, 2023) is a new device that is starting to capture the interest of researchers. It can replace the expansion

**NOMENCLATURE**

| | | | |
|---|---|---|---|
| h | specific enthalpy | *mix* | mixing |
| D | diameter | *prim* | primary |
| $\dot{m}$ | mass flow rate | *sec* | secondary |
| P | pressure | **Acronyms** | |
| T | temperature | COP | Coefficient of Performance |
| **Greeks** | | HP | Heat Pump |
| Δ | difference | HV | Hand Valve |
| $\omega$ | entrainment ratio | MCV | Motor Control Valve |
| **Subscripts** | | NXP | Nozzle Exit Position |
| *c* | compressor | Pl | Pressure Lift |
| *gc* | gas cooler | RTD | Resistance Temperature Detector |

valve while presenting a large capacity to compress. However, a moving rotor with speed control is necessary to manage the flow rates and pressures.

Offering simplicity and cost effectiveness due to no moving components, the ejector emerges as a straightforward and viable alternative for replacing the expansion device and reducing the throttling irreversibility (Aidoun et al., 2019).

In the literature, experimental studies on mechanical compression cycles integrating an ejector as an expander are predominantly focused on $CO_2$ refrigeration applications. Limited experimental studies have explored synthetic refrigerants such as R134a and R410A (Disawas & Wongwises, 2004; Ersoy & Bilir Sag, 2014; Lawrence & Elbel, 2016). For these refrigerants, ejector operation under subcritical conditions is characterized by a relatively low performance and expansion work recovery compared to $CO_2$ applications.

Several experimental studies demonstrated the advantages of integrating a two-phase ejector as an expansion device in $CO_2$ refrigeration systems. Depending on the system design and considered operating conditions, the improvement in COP generally is in the range of 7–20% (Akagi et al., 2004; Elbel & Hrnjak, 2008; Lee et al., 2011; Lucas & Koehler, 2012; Haida et al., 2016; Zhang et al., 2020).

Akagi et al. (2004) experimented a $CO_2$ refrigeration cycle with an ejector. The investigation involved varying the temperature of the refrigerant at the outlet of the gas cooler within the range of 35 °C to 45 °C while maintaining an evaporator pressure at 45 bar. The observed enhancement in the COP over the expansion valve baseline system was approximately 11%. The absence of a diffuser in the ejector suggests the potential for enhancing this performance. The authors also highlighted the critical role of the mixing section geometry and its impact on the ejector's performance.

Elbel and Hrnjak (2008) tested a variable throat ejector within a $CO_2$ refrigeration system. The utilization of a needle permits adjustment of the nozzle throat area, thus facilitating control over the gas cooler pressure. The results revealed that use of the needle led to a reduction in ejector efficiency due to flow disturbance, leading to increased internal losses. Nevertheless, the enhancement in cycle performance and the maximization of COP outweighed the degradation in the ejector's efficiency. Under the tested conditions, the authors observed that integrating the ejector into the cycle resulted in improved cooling capacity and COP, with enhancements of up to 8% and 7–18%, respectively, compared to a basic cycle with an expansion valve.

In an experimental investigation, Lucas and Koehler (2012) carried out a comparative analysis between the $CO_2$ ejector refrigeration cycle and the conventional expansion valve cycle. The evaporating temperature ranged from -10 °C to 1 °C, while the gas cooler outlet temperature extended from 30 °C to 40 °C. The study observed a maximum COP improvement of 17%, complemented by an ejector efficiency reaching up to 22%. Note that the high-pressure side was controlled by modulating the compressor's speed.

The literature on the integration of a two-phase ejector as an expander in $CO_2$ systems for heating applications is relatively sparse compared to refrigeration studies. The high temperature at the gas cooler outlet in heating applications could yield large benefits in ejector utilization (Boccardi et al., 2017); however, there are variable operating conditions that pose challenges for ejector design and its operation close to high efficiency.

Minetto et al. (2013) conducted experiments using a commercially available water-to-water $CO_2$ heat pump, which was adapted to include a two-phase ejector as an expander. Tests were performed at typical hot tap water and space heating conditions. The results presented by the authors indicate a significant ejector entrainment ratio within the range of 0.8-1.6, accompanied by a maximum pressure lift of 5 bar. The ejector enhanced refrigerant circulation in the evaporator and the overall comparison with a conventional heat pump using an expansion valve were favorable, as the isenthalpic process presented increased throttling exergy losses. The authors identified a potentially problematic issue in lubricant recovery.

Xu et al. (2012) conducted an experimental study to control the high-side pressure of a transcritical $CO_2$ ejector heat pump by adjusting the nozzle throat area with a needle. The experimental results led to the formulation of a correlation between the optimal high-side pressure and the gas cooler outlet temperature. The calculated optimal pressure exceeded the values obtained by Elbel and Hrnjak (2008). The authors explained this difference by the absence of an internal heat exchanger in their experimental system.

Boccardi et al. (2017) conducted an experimental study on a $CO_2$ multi-ejector heat pump designed for space

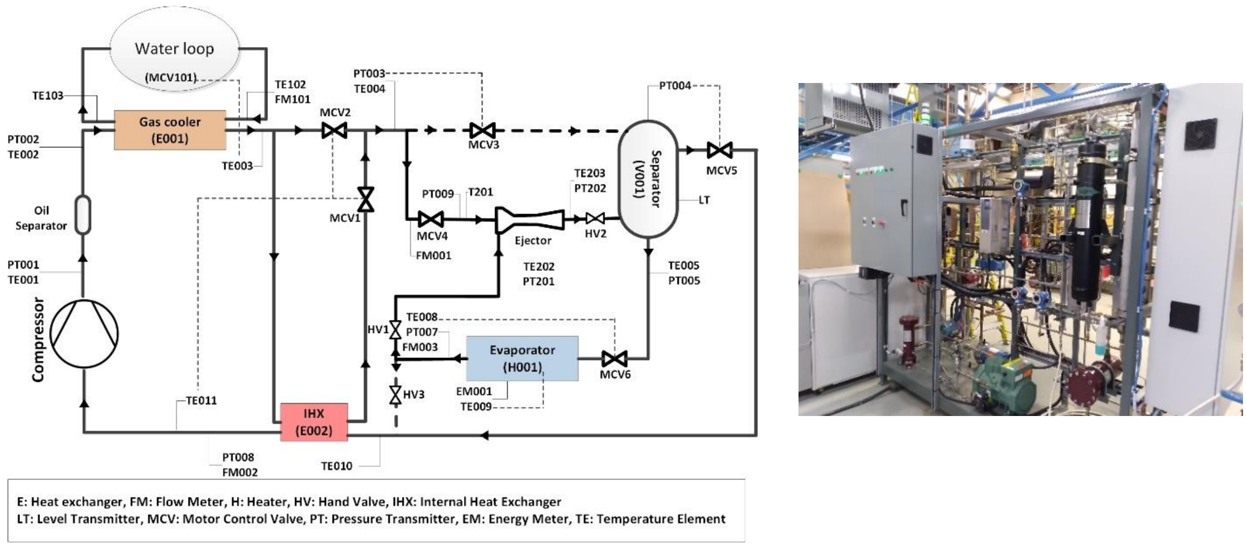


(a) (b)

**Fig. 1 Test bench: (a) simplified schematic, (b) photo**

heating. The incorporation of a multi-ejector pack facilitated the modulation of the ejector cross-section in concordance with operational conditions and load requirements. The results indicate the presence of an ambient temperature threshold, requiring a transition from one ejector to another to optimize system performance. Under specific test conditions, adjusting the multi-ejector throat section enhanced both the COP and the heating capacity by 13.8% and 20%, respectively.

In their experimental study, Zhu et al. (2018) assessed the performance of a transcritical $CO_2$ heat pump water heater, using an ejector with fixed geometry as an expander. Various working conditions were tested, including compressor speed, compressor discharge pressure, expansion valve opening, and water outlet temperature. The ambient and water inlet temperatures were maintained at a constant 22 °C and 20 °C, respectively, while varying the water outlet temperatures in the range of 50–90 °C. The authors observed that incorporating an ejector into the transcritical $CO_2$ heat pump system provides greater benefits in generating high-temperature hot water compared to the basic system. The ejector heat pump achieved a COP of 4.6, which reflects a 10.3% enhancement over the basic cycle, for producing water at 70 °C.

In the literature, most experimental investigations of vapor compression systems with ejectors predominantly focus on refrigeration and air conditioning applications. Generally, the performance enhancements presented occur under conditions of high ejector efficiencies, with different control methods (Zhang et al., 2020).

The proposed research aims to provide new experimental data and insights relevant to heating applications, which are relatively less commonly explored. The focus will be on the interaction between a passive ejector and the compressor and its impact on performance.

This study intends to experimentally investigate the behavior and benefits of integrating a passive two-phase ejector as an expansion device in a $CO_2$ transcritical heat pump operating under various conditions. The basic system with an expansion valve was also tested as a baseline for comparison.

As a first step, two ejectors designed with different modeling approaches were tested separately under the same conditions ($T_{evap}$ = -5 °C, $T_{gc\text{-}out}$ = 35 °C) to identify the best-performing one for subsequent tests. This step evaluated the relevance of combining two different numerical approaches in the design process to optimize ejector performance. The investigation also explored the positioning of the nozzle relative to the mixing chamber, seeking to identify the optimal configuration.

The subsequent investigation focused on evaluating the effects of various evaporating temperatures ($T_{evap}$ = -10 to 0 °C) and $CO_2$ temperatures at the gas cooler's outlet ($T_{gc\text{-}out}$ = 29-38 °C). Conducted under a constant compressor speed, this analysis aimed to understand their influence on the ejector, specifically focusing on entrainment and compression aspects, as well as their impact on the compressor and the heat pump's performance overall.

## 2. EXPERIMENTAL FACILITY

This section provides details on the test bench setup, the tested ejectors, and the measurements including an uncertainty analysis.

### 2.1 Test bench

Figure 1 illustrates the test bench designed and built at CanmetENERGY in Varennes. The facility allows the testing of two applications: a basic transcritical $CO_2$ heat pump that serves as a reference and the same heat pump with an integrated two-phase ejector used as an expansion device instead of the high-pressure valve.

The test bench comprises appropriate components and instrumentation, presenting two loops: a main loop utilizing $CO_2$ as the refrigerant and a secondary water loop connected to the gas cooler. Due to the high pressures involved, stainless steel was predominantly used for the $CO_2$ side's pipes and fittings.

The main components in the $CO_2$ loop include a compressor, an oil separator ensuring adequate lubrication, a gas cooler, a separator, an ejector, an evaporator, and an internal heat exchanger (IHX) to maintain an appropriate level of the compressor suction superheat. In Fig. 1a, various manual and motorized valves are depicted, contributing to the operation and control of the experimental rig.

The compressor is a semi-hermetic reciprocating model (3.3 $m^3$/h at 50 Hz) with variable speed drive. The heat exchangers are the flat plate type. An electrical heater of 10 kW, directly in contact with the refrigerant, is used as an evaporator. This setup eliminates the need for an additional secondary loop to supply heat, simplifying installation and reducing potential heat transfer losses. The heater cast temperature control allows for setting the desired evaporating pressure. The expansion valve (MCV6) located upstream of the evaporator allows for imposing a slight superheat, which is necessary for accurate flow meter measurements. The secondary water loop, not detailed in Fig. 1a, is dedicated to removing heat from the gas cooler and controlling temperature. It essentially consists of a portable circulation chiller with R513 as the refrigerant, along with a pump and valves.

Details regarding the operation of the ejector integrated as an expander in a transcritical $CO_2$ heat pump are well described in a previous paper (Ameur & Aidoun, 2021). In summary, the ejector recovers some of the expansion work to generate a pre-compression by increasing the suction pressure that enhances the performance of the compressor and the overall cycle. The $CO_2$ at high-pressure from the gas cooler flows through the IHX to the ejector, undergoing expansion in the primary nozzle (Fig. 2). This expansion creates favourable conditions for drawing vapor at low pressure from the evaporator. The primary flow and secondary flow mix in the ejector's mixing chamber and undergo compression, which is further enhanced in the diffuser. The ejector discharges a two-phase $CO_2$ mixture at an intermediate pressure into the separator. The saturated vapor from the separator is directed to the compressor suction through the IHX, then it undergoes compression and cooling in the gas cooler. The liquid from the separator expands and evaporates before reaching the secondary inlet of the ejector.

In ejector mode (Fig. 1a), there is no active control of the high-pressure side. Valve MCV4 is fully open and the high-pressure is determined by the primary nozzle inlet conditions and the ejector's geometry. The condition in the separator is also imposed by the ejector discharge performance with the MCV5 valve fully open.

A set of valves is used to allow for switching to the basic heat pump without the ejector. Valves MCV4, HV1, and HV2 are closed to isolate the ejector. The two dashed lines in Fig. 1a are activated by fully opening valves MCV3 and HV3. In the basic heat pump configuration, the high-pressure and intermediate separator pressure are

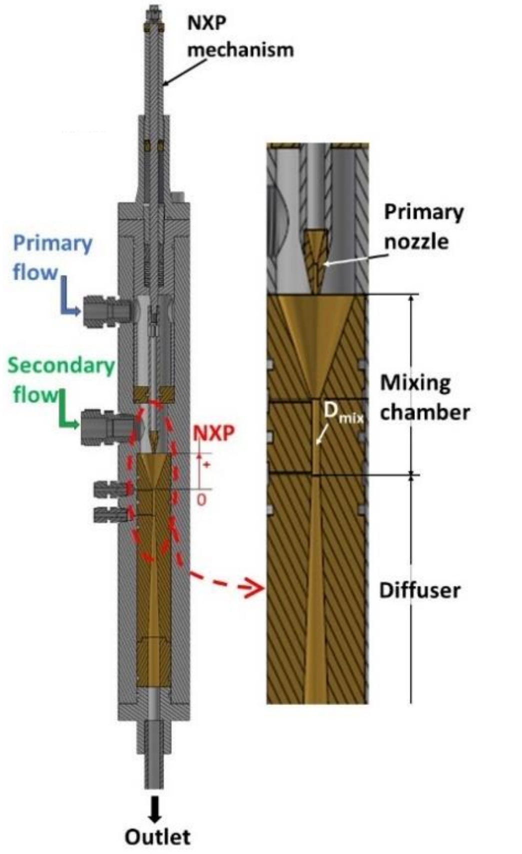


(a) (b)

**Fig. 2 Tested ejector: (a) cross-section view (b) zoom on the mixing chamber**

actively controlled by high-pressure valve MCV3 and flash gas bypass valve MCV5. During the tests on the basic HP, the gas cooler pressure is actively controlled to achieve optimal pressure based on the correlation provided by Sarkar et al. (2004).

### 2.2 Ejector

The ejector (Fig. 2) is a static device with no moving parts, mainly composed of a primary nozzle, a mixing chamber, and a diffuser. The ejector is activated by the high-pressure refrigerant (primary flow), which expands through the convergent-divergent primary nozzle. The variation in the nozzle's cross-section transforms pressure energy into kinetic energy, accelerating the flow to supersonic speeds. This process creates a low-pressure zone at the nozzle outlet, facilitating the entrainment of a low-energy secondary fluid. Primary and secondary flows mix within the mixing chamber, resulting in a complex flow characterized by a shock train structure, which leads to flow deceleration and pressure augmentation. The subsonic flow resulting from this phase undergoes further deceleration and compression in the divergent shape of the diffuser.

Two ejectors were designed for the same heat pump conditions: compressor frequency of 35 Hz, $CO_2$ gas cooler outlet temperature of 35 °C, and an evaporating temperature of -5 °C. These conditions correspond to a primary and secondary pressure of 86.6 bar and 30.4 bar,

**Table 1 Main ejector diameters (in mm)**

| Primary nozzle | | | Mixing out | Diffuser out |
|---|---|---|---|---|
| In | Throat | Out | | |
| 5.9 | 1.08 | 1.3 | 2.7 (Ejec1)<br>2.9 (Ejec2) | 10.54 |

respectively. The first ejector (Ejec1) was designated with a thermodynamic approach; the detailed procedure is reported in a previous paper (Ameur & Aidoun, 2023). The second ejector (Ejec2) is an improved version of the first one, where a CFD approach was used and resulted in an enlarged mixing diameter $D_{mix}$ (Fig. 2). Both ejectors have identical mixing chamber lengths, with the constant diameter section measuring 20 mm. The main diameters of the ejectors are reported in Table 1. Other geometrical parameters, such as angles, can be found in the reference (Ameur & Aidoun, 2023).

The ejectors were manufactured using a modular approach, as illustrated in Fig. 2, which facilitates machining processes and reduces costs. The nozzle, mixing chamber, and diffuser components are made of brass encased in a steel envelope. Appropriate O-rings, selected for compatibility with $CO_2$, are placed at specific locations within the ejector to prevent refrigerant leaks.

Additionally, the ejector features a useful mechanism for adjusting and changing the primary nozzle position (NXP) during test bench operations. The NXP length (the distance between the nozzle output and the mixing chamber with a constant diameter, as depicted in Fig. 2) is rendered dimensionless by the mixing chamber diameter ($D_{mix}$).

### 2.3 Measurements

The locations of the measuring instruments (temperature, pressure, flow rates, electrical power) are illustrated in Fig. 1. The $CO_2$ loop is equipped with three mass flow meters: one at the ejector's primary inlet, one at the evaporator outlet, and one at the compressor suction. The facility includes RTDs temperature sensors, Coriolis flow meters for $CO_2$, a magnetic flow meter for water, piezoresistive pressure sensor with metallic membrane, and a wattmeter. Table 2 shows the measurement uncertainties for the instruments. Data were collected every second and averaged over a 20-minute scan once steady-state conditions were attained. A steady state in the test bench is reached when the pressure and temperature change minimally over a 40-minute observation period.

### 2.4 Data Reduction and Uncertainty Analysis

The key performance metrics for the ejector include the entrainment ratio, ω (Eq. 1), which measures the ejector's capability to draw in the low-pressure fluid, and the pressure lift, Pl (Eq. 2), which evaluates the ejector's ability to increase the pressure of the entrained secondary fluid.

$$\omega = \frac{\dot{m}_{sec}}{\dot{m}_{prim}} \tag{1}$$

$$Pl = P_{out} - P_{sec} \tag{2}$$

$\dot{m}_{prim}$ and $\dot{m}_{sec}$ represent the mass flow rates at the primary and secondary inlets, respectively. $P_{out}$ is the ejector discharge pressure, and $P_{sec}$ is the pressure at the ejector's secondary inlet (evaporating pressure).

Equations 3-5 represent the main performance indicators used to characterize the heat pump system: the heating capacity of the gas cooler ($Q_{gc}$), the compressor power ($W_c$), and the coefficient of performance for heating (COP). The evaporator capacity ($Q_{evap}$) was measured by the wattmeter.

$$Q_{gc} = \dot{m}_c\, \Delta h_{gc} \tag{3}$$

$$W_c = \dot{m}_c\, \Delta h_c \tag{4}$$

$$COP = \frac{Q_{gc}}{W_c} \tag{5}$$

Where $\dot{m}_c$ represents the compressor mass flow rate, $\Delta h_{gc}$ denotes the difference in specific enthalpy across the gas cooler, and $\Delta h_c$ is the difference in specific enthalpy across the compressor.

The gas cooler capacity evaluated on the $CO_2$ side was compared with that obtained from measurements on the water side. An average difference of 1.2% was observed, indicating good insulation of the gas cooler with negligible heat loss.

Equation 5 is valid for evaluating the COP of both systems: the basic one and the ejector system. The difference (ΔCOP), evaluated with Eq. (6), is used to quantify the contribution of the ejector compared to the basic heat pump.

$$\Delta COP = 100 \times \frac{COP_{ejec} - COP_{basic}}{COP_{basic}} \tag{6}$$

Considering the precision of the measurement instruments and following the classical method of Kline and McClintock (ASHRAE Guideline 2, 1986), the uncertainty calculations associated with ω, Pl, $Q_{gc}$, $Q_{evap}$, $W_c$, and COP were 0.75%, 1.77%, 2.1%, 1.4%, 1.3%, and 2.35%, respectively.

**Table 2 Instrument uncertainties**

| Variable | Instrument type | Uncertainty | Range |
|---|---|---|---|
| Refrigerant mass flow rate | Coriolis flow meter | ± 0.75% | 0–60 g/s |
| Water flow rate | Magnetic flow meter | ±0.5% | 0–30 l/min |
| Temperature | Resistance detector | ±0.15 °C | -15–70 °C |
| Pressure | Piezoresistive sensor | ±0.08% | 0–100 bar |
| Electrical power | Wattmeter | ±1.4% | 0–20 kW |

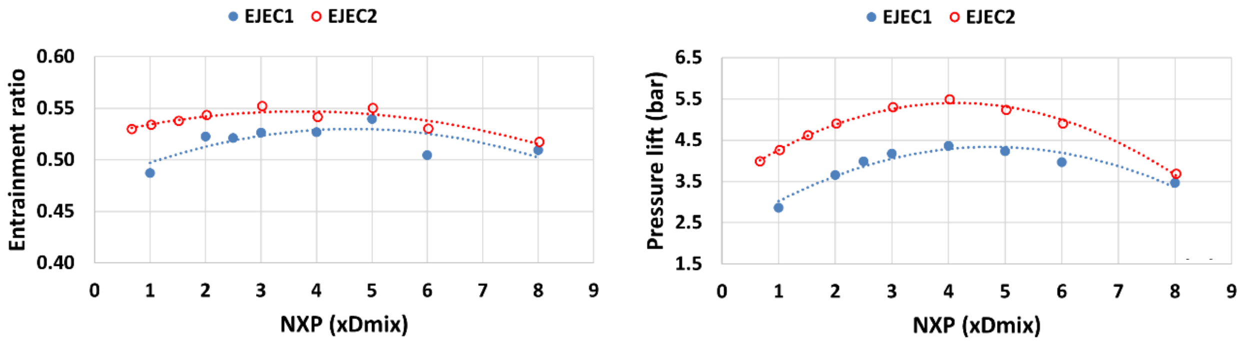


(a) (b)

**Fig. 3 NXP effects on: (a) the entrainment ratio and (b) the pressure lift**

## 3. RESULTS AND DISCUSSION

In this section, the results are presented in three parts. The first part involves a comparison of two ejectors, Ejec1 and Ejec2, each with different mixing diameters, under the same evaporating and gas cooler conditions. The objective is to identify the most efficient ejector for subsequent tests. Additionally, during this initial phase, the NXP is investigated.

The second part of the results examines the influence of evaporating temperature on the ejector's behavior and its subsequent impact on the heat pump's performance. In the third part, the effect of the $CO_2$ gas cooler outlet temperature is analyzed. A comparison with the conventional heat pump is conducted to illustrate the advantages of employing a two-phase ejector as an expander, for the design conditions ($T_{gc\text{-}out}$ = 35 °C, $T_{evap}$ = -5 °C) as well as for other conditions.

Throughout all tests, the compressor operates at a constant frequency of 35 Hz with a suction superheat of 10 K. A superheating of about 5 K is maintained at the evaporator outlet to ensure accurate flow rate measurement. Lawrence and Elbel (2019) maximized the heating COP in their ejector HP experiment by imposing no superheat at the evaporator outlet. However, they observed that a superheat of 5 K has a negligible impact on the COP.

### 3.1 Ejec1 vs. Ejec2 with NXP variation

Figure 3 presents the effects of NXP variation (0.65-8$D_{mix}$) on the entrainment ratio and pressure lift of two ejectors, Ejec1 and Ejec2, under the same conditions ($T_{evap}$ = -5 °C, $T_{gc\text{-}out}$ = 35 °C).

Overall, for the two tested ejectors, the NXP variation maximizes performance (entrainment and pressure lift) in the range of 3-5$D_{mix}$, with a clear peak at 4$D_{mix}$ for the pressure lift (Fig. 3b). The pressure lift appears to be more sensitive to the nozzle position compared to entrainment (Fig. 3a), which shows a relatively flatter variation. Therefore, by adjusting the nozzle closer to the mixing chamber (reducing the NXP from 4$D_{mix}$ to 1$D_{mix}$), the pressure lift of the two ejectors is reduced by approximately more than 1.5 bar.

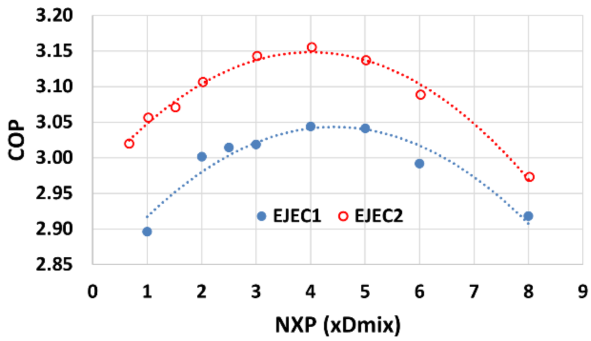


**Fig. 4 NXP effects on the COP**

Explaining the effect of nozzle displacement on the ejector's performance is challenging without internal flow visualization. The structure of the jet at the nozzle exit is most likely affected by this displacement. Furthermore, as the primary nozzle is positioned near the mixing chamber with a constant diameter, it results in a growing obstruction of the secondary flow passage. However, in the case of a nozzle positioned far from the mixing chamber, it is probable that the expansion of the jet and its structure disrupt the secondary flow passage.

The heat pump's heating COP is sensitive to the ejector nozzle's position (Fig. 4). In the case of Ejec2, moving the nozzle from an NXP of 4$D_{mix}$ to 1$D_{mix}$ reduces the COP by around 3.5%. Note that COP maximizing occurs within the same range of NXP (3-5$D_{mix}$) as for the ejector's performance. Liu et al (2016), in their experiment with a $CO_2$-based air-conditioning system, achieved COP maximization at a NXP of approximately 3$D_{mix}$.

Figures 3 and 4 also show that Ejec2, with its larger mixing diameter, outperforms Ejec1. At the NXP position of 4$D_{mix}$, Ejec2 presents a slight entrainment improvement (+2.6%) with higher improvement for the pressure lift (+25.6%), resulting in a COP improvement of 3.9%.

Increasing ejector performance with a larger mixing diameter is probably due to a reduced pressure drop and an enhanced mixing process. However, a limited pressure drop reduction is expected due to the friction caused by the low viscosity of $CO_2$, and the impact of improved mixing will probably be more significant. Improved mixing of the primary and secondary flows results in a

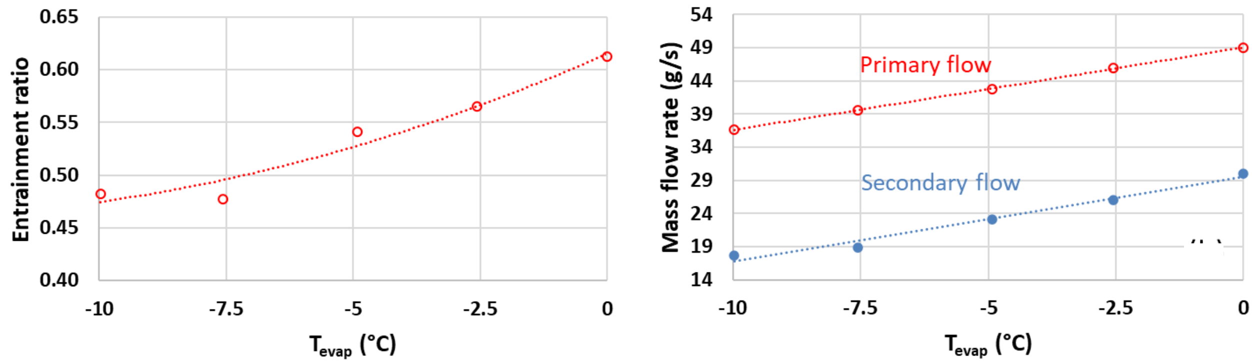


(a) (b)

**Fig. 5 Ejector entrainment performance variation with $T_{evap}$: (a) entrainment ratio (b) mass flow rates**

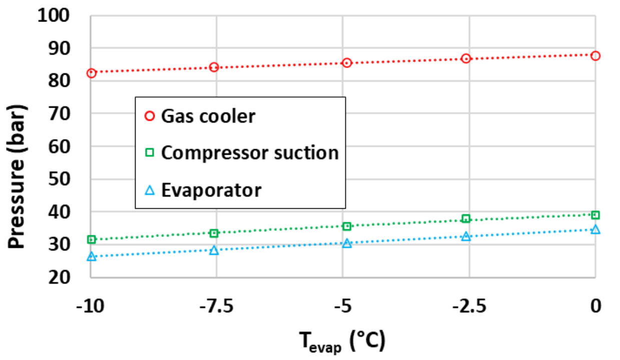


**Fig. 6 Pressures in the ejector HP as a function of evaporating temperature**

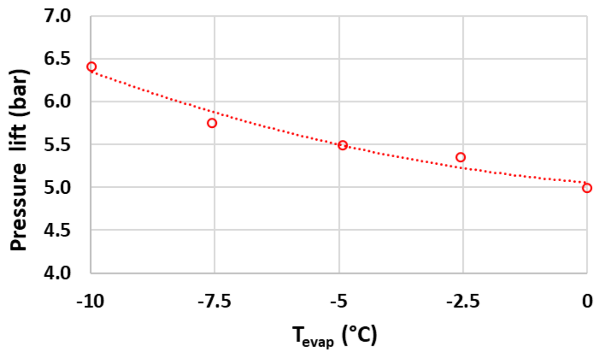


**Fig. 7 Ejector's pressure lift variation with evaporating temperature**

more efficient transfer of momentum and an overall enhancement in diffuser efficiency, positively impacting pressure recovery.

Finally, ejector Ejec2 with NXP=4$D_{mix}$ as the optimal nozzle position is selected for the rest of the results.

### 3.2 Effect of the Evaporating Temperature

In this section, the behavior of the ejector and its impact on the heat pump performance is examined under different evaporating temperatures (-10 °C to 0 °C) with a constant $T_{gc\text{-}out}$ (35 °C).

Figure 5 illustrates the variation of the entrainment ratio, as well as the primary and secondary mass flow rates at different evaporating temperatures.

The decrease in the ejector entrainment ratio with a lower evaporating temperature (Fig. 5a) is attributed to a reduction in the primary and secondary mass flow rates (Fig. 5b). As the $T_{evap}$ decreases, the pressure in both the evaporator and the gas cooler decreases (Fig. 6). Despite that the ejector's pressure lift increases (Fig. 7) with a lower $T_{evap}$, the result is a lower pressure at the compressor suction and a higher compression ratio. Consequently, the primary mass flow rate decreases, reducing the energy in the motive flow and resulting in a lower induced secondary flow. Boccardi et al. (2017) observed the same trend in the ejector behavior with decreasing ambient temperature.

Figure 7 presents the changes in the ejector's pressure lift with varying evaporating temperatures. As the $T_{evap}$ decreases from 0 °C to -10 °C, the ejector exhibits higher compression, resulting in an increase in pressure lift from 5 bar to 6.5 bar. Note that this increase is nonlinear; the slope of the curve steepens at lower temperatures. In summary, lowering the evaporating temperature reduces the ejector's entrainment performance while enhancing its compression capacity.

Figure 8 illustrates the changes in gas cooler capacity, evaporator capacity, and compressor power with varying evaporating temperatures for both the basic and ejector cycles. Note the expected trend of capacity degradation as evaporating temperatures drop. However, the use of an ejector clearly enhances the gas cooler and evaporator capacities compared to the basic HP with an expansion valve, as shown in Fig. 8a-b, with almost the same compressor power (Fig. 8c). Hence, at $T_{evap}$ = -5 °C, the ejector improves the gas cooler and evaporator capacities by 20.5% and 17.5%, respectively.

The heating COP and difference ΔCOP variation with $T_{evap}$ are presented in Fig. 9. For the tested $T_{evap}$, the heat pump with ejector presents a higher COP than the basic system (Fig. 9a). At $T_{evap}$ = -5 °C, the ejector improves the COP by 18%, with a slight decrease at the other temperatures (Fig. 9b). Even though the ejector was initially designed for an evaporating temperature of -5 °C, results show that the ejector's performance improvement extends beyond this temperature.

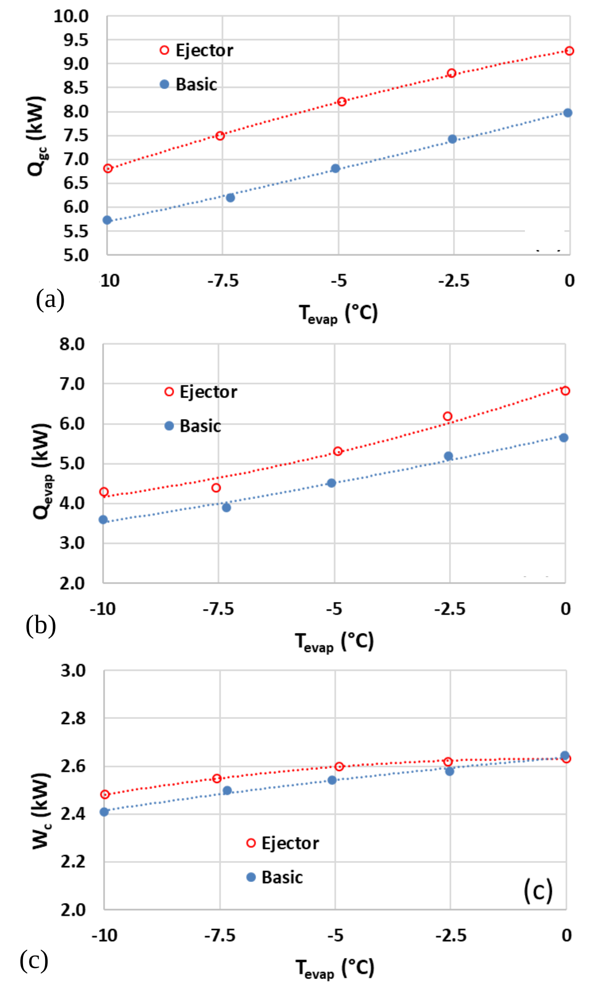


**Fig. 8 (a) $Q_{gc}$ (b) $Q_{evap}$ (c) $W_c$ variation with $T_{evap}$ for the basic and ejector cycles**

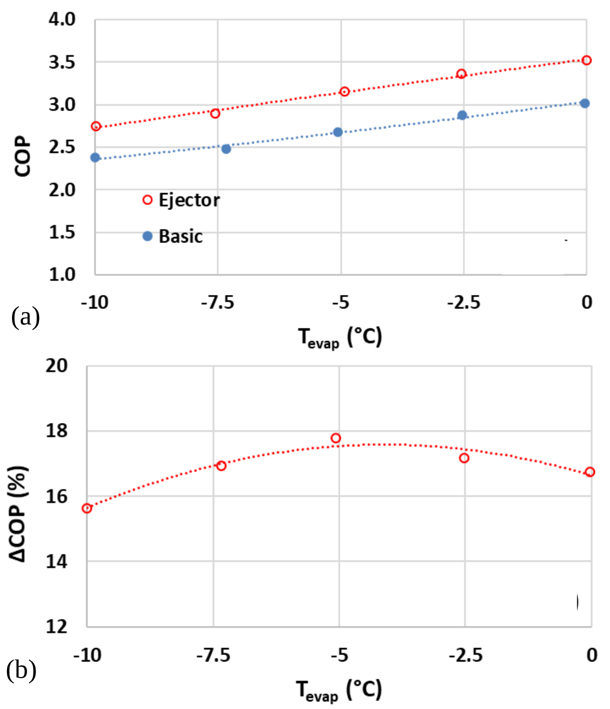


**Fig. 9 (a) COP and (b) ΔCOP variation with evaporating temperature**

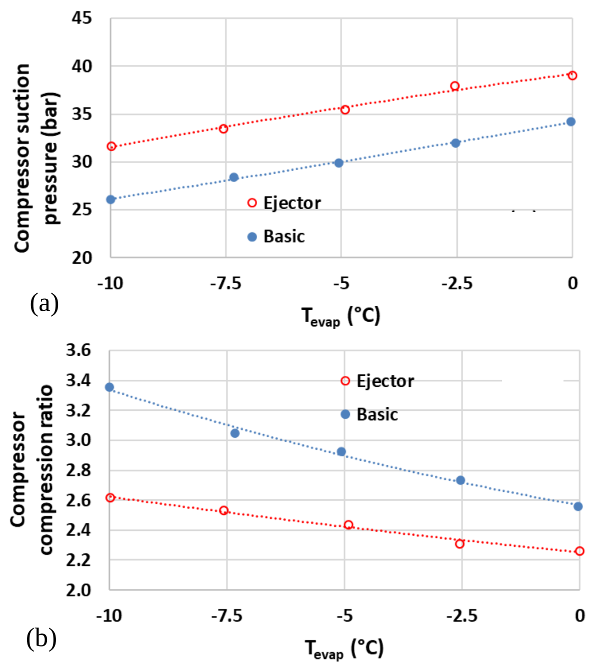


**Fig. 10 (a) compressor suction pressure and (b) compressor ratio pressure variation with $T_{evap}$ for the basic and ejector cycles**

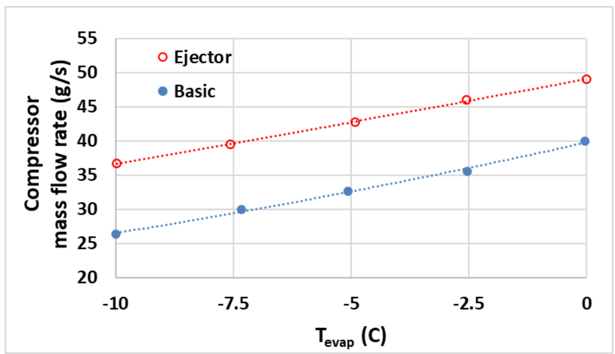


**Fig. 11 Compressor mass flow rate variation with $T_{evap}$ for the basic and ejector cycles**

Figure 10 illustrates the changes of the compressor suction pressure and the compression ratio with respect to the $T_{evap}$ for both the basic and ejector cycles. The ejector impacts the compressor by increasing the suction pressure (Fig. 10a), hence reducing its compression ratio (Fig. 10b), resulting in an improvement in the compressor's performance relative to the basic cycle. This ejector effect, among others, enables a higher mass flow rate through the compressor compared to the basic cycle, as illustrated in Fig. 11.

### 3.3 Effect of Gas Cooler Temperature

In this section, the investigation focuses on the impact of varying $CO_2$ gas cooler outlet temperatures (ranging from 29 °C to 38 °C) on the ejector performance and the heat pump performance, considering a constant evaporating temperature (-5 °C) and constant compressor speed (35 Hz).

Figure 12 presents the changes in the ejector entrainment ratio, as well as the primary and secondary

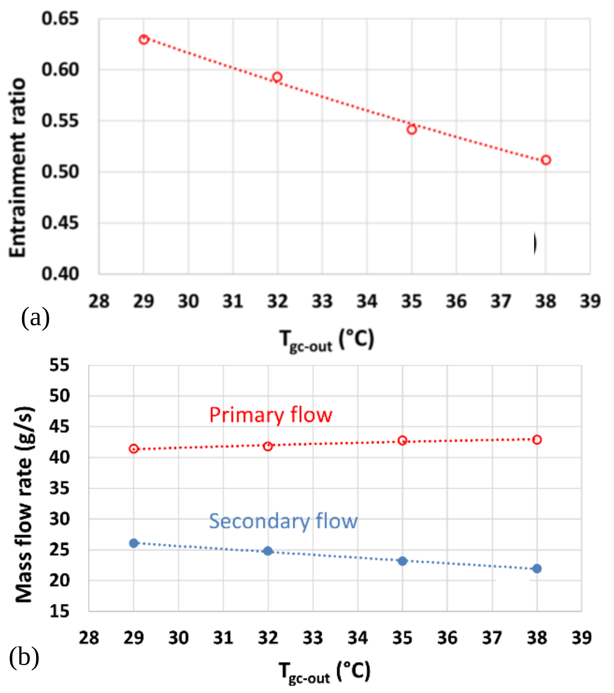


**Fig. 12 Ejector entrainment performance variation with $T_{gc\text{-}out}$: (a) entrainment ratio (b) mass flow rates**

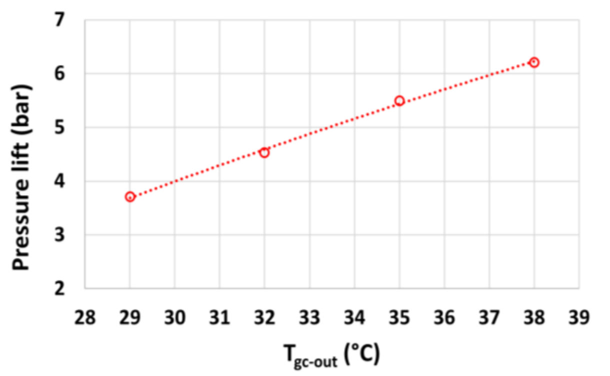


**Fig. 13 Ejector's pressure lift variation with $T_{gc\text{-}out}$**

flow rates at different gas cooler temperatures. As the $T_{gc\text{-}out}$ decreases from 38 °C to 29 °C, the ejector entrainment ratio increases by 23%. This improvement is due to the significant increase in secondary flow (+18.4%) (Fig. 12b). The variation of the ejector's pressure lift with respect to the gas cooler temperature is presented in Fig. 13. As the $T_{gc\text{-}out}$ decreases from 38 °C to 29 °C, the pressure lift decreases from 6.2 bar to 3.7 bar, representing a reduction of nearly 40%. In their experiment on ejector $CO_2$ refrigeration, Akagi et al. (2004) demonstrate a similar trend in both ejector entrainment ratio and pressure lift when varying the nozzle inlet temperature.

Varying $T_{gc\text{-}out}$ has a direct impact on the ejector motive flow inlet (i.e., the nozzle inlet). As the $T_{gc\text{-}out}$ decreases, $CO_2$ properties at the inlet of the ejector's primary nozzle change drastically, especially approaching critical condition and reaching sub-critical condition. This weakens the ejector's capacity to compress, as observed in Giacomelli's (2019) experiment.

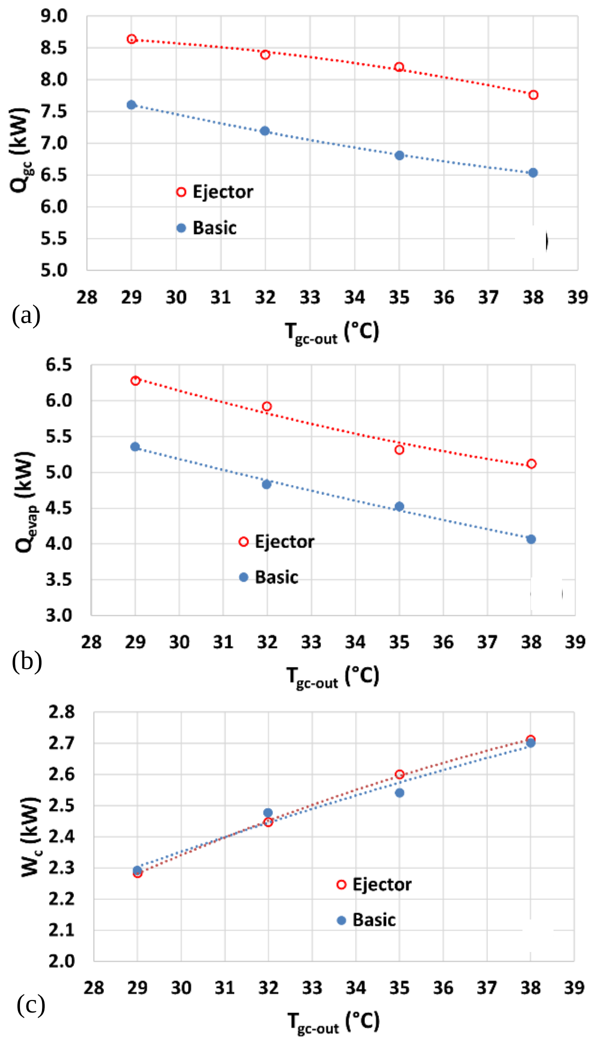


**Fig. 14 (a) $Q_{gc}$ (b) $Q_{evap}$ (c) $W_c$ variation with $T_{gc\text{-}out}$ for the basic and ejector cycles**

Figure 14 illustrates the changes in gas cooler capacity, evaporator capacity, and compressor power with respect to the gas cooler temperature for both the basic and ejector cycles. In general, a decrease in the $CO_2$ gas cooler temperature results in improved heat pump capacities and reduces compressor power. As the $T_{gc\text{-}out}$ decreases, the gas cooler pressure reduces. This is achieved by controlling the high-pressure valve for the basic cycle and through the ejector's passive effect in the ejector cycle. Thus, approaching critical conditions results in significant improvements in the specific heat capacity of $CO_2$, as indicated by Bastani et al. (2020), and ultimately enhancing gas cooler capacity (Fig. 14a). Lowering the $T_{gc\text{-}out}$ increases the $CO_2$ mass flow rate in the evaporator, thus enhancing heat extraction as depicted in Fig. 14b. Reducing the compressor discharge pressure with low $T_{gc\text{-}out}$ results in lower compressor power (Fig. 14c).

Figures 14a-b also show that the integration of an ejector enhances the capacities of the transcritical $CO_2$ heat pump compared to the basic cycle, while presenting the same compressor work (Fig. 14c). Note that the positive impact of the ejector on heat pump capacities tends to diminish as the gas cooler temperature is reduced.

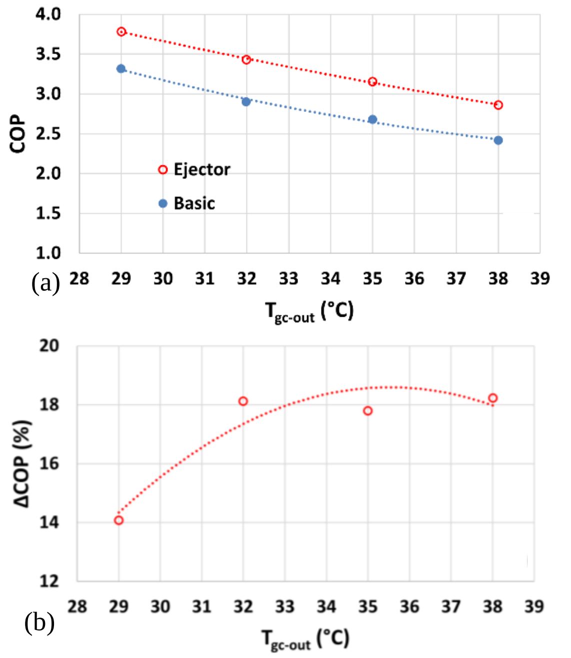


**Fig. 15 (a) COP and (b) ΔCOP variation with $T_{gc-out}$**

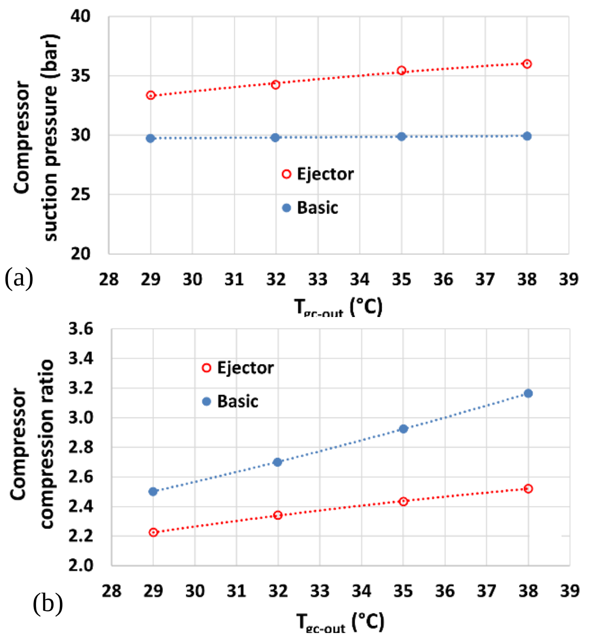


**Fig. 16 (a) compressor suction pressure and (b) compressor ratio pressure variation with $T_{gc-out}$ for the basic and ejector cycles**

At $T_{gc-out}$ = 38 °C, the ejector improves the gas cooler and evaporator capacities by 18.6% and 26%, respectively, compared to the basic cycle. These improvements decrease to 13.6% and 17.1%, respectively, when the $T_{gc-out}$ is reduced to 29 °C. This trend is confirmed by the heating COP variation as a function of $T_{gc-out}$ in Fig. 15. The ejector improves COP by almost 18%, except at the subcritical gas cooler temperature (29 °C), where the improvement is reduced to 14%.

The enhanced performance of the heat pump with the ejector, as compared to the basic cycle, is a result of the pressure lift generated by the ejector. This pressure lift improves compressor suction pressure, as shown in Fig. 16a. Note that in the basic cycle, the suction pressure is slightly lower than the evaporator pressure, mainly due to pressure drops occurring in the suction line. Figure 16b illustrates the effect of the ejector's pressure lift in reducing the compressor compression ratio, thereby enhancing compressor operation. Finally, Fig. 16 illustrates the diminishing influence of the ejector with a decreasing $T_{gc-out}$ due to the decline in pressure lift. This trend explains the degradation of ΔCOP as the $T_{gc-out}$ decreases, as observed above.

## 4. Conclusion

An experimental investigation was carried out on a transcritical $CO_2$ heat pump featuring a passive two-phase ejector integrated as an expander. The investigation examined the effects of changes in evaporating temperature and $CO_2$ gas cooler outlet temperature on the performances of both the ejector and the overall cycle. The performance was compared to the basic heat pump with an expansion valve.

First, the significance of combining two different numerical approaches in the ejector design was evaluated. Two ejectors were tested: Ejec1, designed with thermodynamic modeling, and Ejec2, further refined through the CFD approach. Ejec2, with a larger mixing diameter, exhibited enhanced performance, particularly in compression, achieving an additional one bar in pressure lift, resulting in a 3.9% improvement in COP. The optimal nozzle position (NXP) was identified as $4D_{mix}$, maximizing both the ejector and overall system performances.

Although the ejector was designed for specific conditions, the results demonstrate the ejector's flexibility and ability to remain operational under varying conditions with some changes in performance.

The results indicate that with a decrease in evaporating temperature, the ejector's entrainment ratio decreases, while the pressure lift increases, reaching a maximum of 6.5 bar at $T_{evap}$ = -10 °C. Under the tested evaporating temperatures, the integration of the ejector enhances the heat pump performance, particularly regarding capacity. When compared to the basic heat pump at $T_{evap}$ = -5 °C, the ejector demonstrates improvements in the gas cooler's capacity, the evaporator's capacity, and the COP, of 20.5%, 17.5%, and 17.8%, respectively. Furthermore, the same ejector, tested at $T_{evap}$ = -10 °C and 0 °C, still exhibited enhanced performance, with a ΔCOP of approximately 16%.

The performance of the ejector is notably influenced by the $CO_2$ gas cooler outlet temperature, which alters the inlet conditions of the motive fluid. Decreasing the gas cooler temperature results in an increase in ejector entrainment, along with a decrease in pressure lift, reaching 3.7 bar at $T_{gc-out}$ = 29 °C. The positive impact of the ejector on the heat pump's capacities and COP tends to diminish as the gas cooler temperature is reduced to subcritical conditions. At $T_{gc-out}$ = 38 °C, compared to the basic cycle, the ejector enhances the gas cooler's capacity, the evaporator's capacity, and the COP by 18.6%, 26%, and 18%, respectively. These improvements decrease to 13.6%, 17.1%, and 14%, respectively when the $T_{gc\text{-}out}$ is reduced to 29 °C.

Finally, the study highlighted the detailed interaction between the ejector and the compressor. This insight is crucial for understanding the impact of the ejector on system performance. The ejector cycle improvement is primarily based on improved mass flow rates resulting from increased compressor suction pressure, reduced compression ratio, and consequently improved compressor operating conditions.

## ACKNOWLEDGEMENTS

This project is supported by a Natural Resources Canada research and development program (PERD). The authors wish to thank the technical team at CanmetENERGY in Varennes for their assistance and support.

## CONFLICT OF INTEREST

The authors have no conflicts to disclose.

## AUTHORS CONTRIBUTION

**K. Ameur**: Conceptualization, Methodology, Data, Visualization, Writing. **M. Falsafioon:** Data.

## REFERENCES

Aidoun, Z., Ameur, K., Falsafioon, M., & Badache, M. (2019). Current advances in ejector modeling, experimentation and applications for refrigeration and heat pumps. part 2: two-phase ejectors. *Inventions*, *4*(16), 1–54. https://doi.org/10.3390/inventions4010016

Akagi, S., Wang, J., & Hihara, E. (2004). *Characteristics of two-phase ejector with carbon dioxide.* 41st National Heat Transfer Symposium of Japan.

Ameur, K., & Aidoun, Z. (2021). Two-phase ejector enhanced carbon dioxide transcritical heat pump for cold climate. *Energy Conversion and Management*, *243*, 114421. https://doi.org/10.1016/j.enconman.2021.114421

Ameur, K., & Aidoun, Z. (2023). A Simple design approach of two-phase ejectors for CO2 transcritical heat pumps. *Journal of Applied Fluid Mechanics*, *16*(10), 1887–1900. https://doi.org/10.47176/jafm.16.10.1833

Arpagaus, C., Bless, F., Schiffmann, J., & Bertsch, S. S. (2016). Multi-temperature heat pumps: A literature review. *International Journal of Refrigeration*, *69*, 437–465. https://doi.org/10.1016/j.ijrefrig.2016.05.014

ASHRAE Guideline 2. (1986). *Engineering analysis of experimental data.* American Society of Heating, Refrigerating, and Air-Conditioning Engineers, Inc. https://doi.org/ASHRAE Guideline 2-1986 (RA90)

Badache, M., Ouzzane, M., Eslami-Nejad, P., & Aidoun, Z. (2018). Experimental study of a carbon dioxide direct-expansion ground source heat pump (CO2-DX-GSHP). *Applied Thermal Engineering*, *130*, 1480–1488. https://doi.org/10.1016/j.applthermaleng.2017.10.159

Barta, R. B., Groll, E. A., & Ziviani, D. (2021). Review of stationary and transport CO2 refrigeration and air conditioning technologies. *Applied Thermal Engineering*, *185*(August 2020), 116422. https://doi.org/10.1016/j.applthermaleng.2020.116422

Bastani, A., Eslami-Nejad, P., Badache, M., & Nguyen, A. T. A. (2020). Experimental characterization of a transcritical CO2 direct expansion ground source heat pump for heating applications. *Energy and Buildings*, *212*. https://doi.org/10.1016/j.enbuild.2020.109828

Boccardi, G., Botticella, F., Lillo, G., Mastrullo, R., Mauro, A. W., & Trinchieri, R. (2017). Experimental investigation on the performance of a transcritical CO2 heat pump with multi-ejector expansion system. *International Journal of Refrigeration*, *82*, 389–400. https://doi.org/10.1016/j.ijrefrig.2017.06.013

Disawas, S., & Wongwises, S. (2004). Experimental investigation on the performance of the refrigeration cycle using a two-phase ejector as an expansion device. *International Journal of Refrigeration*, *27*(6), 587–594. https://doi.org/10.1016/j.ijrefrig.2004.04.002

Elbel, S., & Hrnjak, P. (2008). Experimental validation of a prototype ejector designed to reduce throttling losses encountered in transcritical R744 system operation. *International Journal of Refrigeration*, *31*(3), 411–422. https://doi.org/10.1016/j.ijrefrig.2007.07.013

Elbel, S., & Lawrence, N. (2016). Review of recent developments in advanced ejector technology. *International Journal of Refrigeration*, *62*, 1–18. https://doi.org/10.1016/j.ijrefrig.2015.10.031

Ersoy, H. K., & Bilir Sag, N. (2014). Preliminary experimental results on the R134a refrigeration system using a two-phase ejector as an expander. *International Journal of Refrigeration*, *43*, 97–110. https://doi.org/10.1016/j.ijrefrig.2014.04.006

Ferrara, G., Ferrari, L., Fiaschi, D., Galoppi, G., Karellas, S., Secchi, R., & Tempesti, D. (2016). Energy recovery by means of a radial piston expander in a CO2 refrigeration system. *International Journal of Refrigeration*, *72*, 147–155. https://doi.org/10.1016/j.ijrefrig.2016.07.014

Giacomelli, F., Mazzelli, F., Banasiak, K., Hafner, A., & Milazzo, A. (2019). Experimental and computational analysis of a R744 flashing ejector. *International Journal of Refrigeration*, *107*, 326–343. https://doi.org/10.1016/j.ijrefrig.2019.08.007

Haida, M., Banasiak, K., Smolka, J., Hafner, A., & Eikevik, T. M. (2016). Experimental analysis of the R744 vapour compression rack equipped with the multi-ejector expansion work recovery module. *International Journal of Refrigeration*, *64*, 93–107. https://doi.org/10.1016/j.ijrefrig.2016.01.017

Lawrence, N., & Elbel, S. (2016). Experimental investigation on the effect of evaporator design and application of work recovery on the performance of two-phase ejector liquid recirculation cycles with R410A. *Applied Thermal Engineering*, *100*, 398–411. https://doi.org/10.1016/j.applthermaleng.2016.01.079

Lawrence, N., & Elbel, S. (2019). Experimental investigation on control methods and strategies for off-design operation of the transcritical R744 two-phase ejector cycle. *International Journal of Refrigeration*, *106*, 570–582. https://doi.org/10.1016/j.ijrefrig.2019.04.020

Lee, J. S., Kim, M. S., & Kim, M. S. (2011). Experimental study on the improvement of CO2 air conditioning system performance using an ejector. *International Journal of Refrigeration*, *34*(7), 1614–1625. https://doi.org/10.1016/j.ijrefrig.2010.07.025

Liu, F., Groll, E. A., & Ren, J. (2016). Comprehensive experimental performance analyses of an ejector expansion transcritical CO2 system. *Applied Thermal Engineering*, *98*, 1061–1069. https://doi.org/10.1016/j.applthermaleng.2015.12.017

Liu, J., Liu, Y., & Yu, J. (2021). Performance analysis of a modified dual-ejector and dual-evaporator transcritical CO2 refrigeration cycle for supermarket application. *International Journal of Refrigeration*, *131*, 109–118. https://doi.org/10.1016/j.ijrefrig.2021.06.010

Lucas, C., & Koehler, J. (2012). Experimental investigation of the COP improvement of a refrigeration cycle by use of an ejector. *International Journal of Refrigeration*, *35*(6), 1595–1603. https://doi.org/10.1016/j.ijrefrig.2012.05.010

Minetto, S., Brignoli, R., Banasiak, K., Hafner, A., & Zilio, C. (2013). Performance assessment of an off-the-shelf R744 heat pump equipped with an ejector. *Applied Thermal Engineering*, *59*(1–2), 568–575. https://doi.org/10.1016/j.applthermaleng.2013.06.032

Sarkar, J. (2015). Review and future trends of supercritical CO2 Rankine cycle for low-grade heat conversion. *Renewable and Sustainable Energy Reviews*, *48*, 434–451. https://doi.org/10.1016/j.rser.2015.04.039

Sarkar, J., Bhattacharyya, S., & Gopal, M. R. (2004). Optimization of a transcritical CO2 heat pump cycle for simultaneous cooling and heating applications. *International Journal of Refrigeration*, *27*, 830–838. https://doi.org/10.1016/j.ijrefrig.2005.12.006

Sengupta, A., & Dasgupta, M. S. (2023). CFD supported thermodynamic analysis of a CO2 pressure exchanger based refrigeration system for supermarkets. *International Journal of Refrigeration*. https://doi.org/10.1016/j.ijrefrig.2023.04.012

Song, Y., Cui, C., Yin, X., & Cao, F. (2022). Advanced development and application of transcritical CO2 refrigeration and heat pump technology—A review. *Energy Reports*, *8*, 7840–7869. https://doi.org/10.1016/j.egyr.2022.05.233

Wang, J., Belusko, M., Evans, M., Liu, M., Zhao, C., & Bruno, F. (2022). A comprehensive review and analysis on CO2 heat pump water heaters. *Energy Conversion and Management: X*, *15*(July), 100277. https://doi.org/10.1016/j.ecmx.2022.100277

Xu, X. X., Chen, G. M., Tang, L. M., & Zhu, Z. J. (2012). Experimental investigation on performance of transcritical CO2 heat pump system with ejector under optimum high-side pressure. *Energy*, *44*(1), 870–877. https://doi.org/10.1016/j.energy.2012.04.062

Zhang, J. F., Qin, Y., & Wang, C. C. (2015). Review on CO2 heat pump water heater for residential use in Japan. *Renewable and Sustainable Energy Reviews*, *50*, 1383–1391. https://doi.org/10.1016/j.rser.2015.05.083

Zhang, Z., Feng, X., Tian, D., Yang, J., & Chang, L. (2020). Progress in ejector-expansion vapor compression refrigeration and heat pump systems. *Energy Conversion and Management*, *207*(February), 112529. https://doi.org/10.1016/j.enconman.2020.112529

Zhu, Y., Huang, Y., Li, C., Zhang, F., & Jiang, P. X. (2018). Experimental investigation on the performance of transcritical CO2 ejector-expansion heat pump water heater system. *Energy Conversion and Management*, *167*(March), 147–155. https://doi.org/10.1016/j.enconman.2018.04.081